Model Validation of SIM External Metrology at the Sub-Nanometer Level

Bijan Nemati [a] and Gary M. Kuan [a*]

[a] Jet Propulsion Laboratory, 4800 Oak Grove Dr., M/S 301-486, Pasadena, CA, U.S.A.

ABSTRACT

In order to achieve micro-arcsecond astrometry, SIM must make measurements of various optical path lengths at the picometer level. In this regime of precision, nearly every simplifying assumption in optics must be reexamined as a potential source of systematic error. SIM makes extensive use of physics-based models to predict the form and level of systematic errors affecting instrument performance. Since many of the modeling areas represent new frontiers in optical modeling, the validation of these physical models is a significant challenge that SIM must meet. In the case of the external metrology truss, the model must account for the imperfections in the corner cubes as well as the distance measuring interferometers ("beam launchers"). This model is being validated using the Kite testbed, a 2-D metrology truss with picometer-level accuracy in displacement measurements. We present the model and the results of the model validation tests on the Kite testbed.

Keywords: Interferometry, Metrology, Corner Cubes, SIM, Astrometry, Model, Validation, Testbed, Kite

1. INTRODUCTION

The Space Interferometry Mission (SIM) is a multipurpose instrument which is uniquely suited for high-precision astrometry. [2] SIM has two basic modes of astrometric observations: the first is the Narrow-Angle (NA), required to be accurate to 1 μas over 1 degree in the sky, and second is the Wide-Angle (WA), required to be accurate to 4 μas over 15 degrees in the sky. As the instrument's siderostats slew from one star to another, the SIM external metrology system tracks the change in the baselines of the guide and science interferometers.

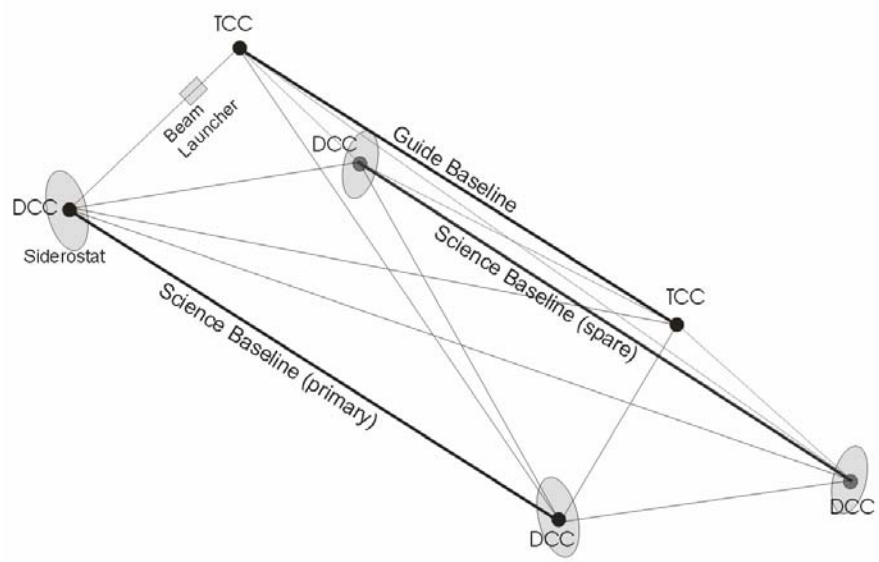

Figure 1: SIM's external metrology truss connects six fiducials, four double corner cubes (DCC) mounted on the science siderostats, and two triple corner cubes (TCC) used by the guide interferometers.

[*] Further author information: (Send correspondence to B.N.)
B.N.: E-mail: bijan.nemati@jpl.nasa.gov, Telephone: 1 818 354 0883
G.M.K.: E-mail: gkuan@jpl.nasa.gov, Telephone: 1 818 393 0270

The design of the instrument is such that these baselines are nominally to stay unchanged. However, in the presence of thermal and vibrational disturbances, as well as mechanical imprecision in the slew mechanisms, there are inevitable changes in the baseline vector. The scale of these changes is of order 1 μrad, while the accuracy to which these need to be known is in the pico radians. It is the function of the external metrology system to provide this knowledge.

The external metrology system, shown in Figure 1, is composed of 6 fiducials and 15 metrology paths monitored by displacement-measuring interferometers called beam launchers. Two of the fiducials are triple corner cubes (TCC) used by the guide interferometers. The design of the guide interferometers is such that the TCC's do not need to be articulated during any observations. The science interferometers, however, require siderostats to articulate over a radius of 3.75 degrees to cover 15 degrees in the sky. Mounted on each siderostat is a double corner cube (DCC) which articulates along with it. The interferometers must measure the starlight path length difference (through one arm versus the other) while tracking baseline changes. The guide baseline is the vector connecting the two TCC's and the science baseline vector connects the two TCC's. There is a redundant, secondary science interferometer whose DCC's do not articulate during normal observations.

When the DCC is articulated over the SIM-required field of regard, a field-dependent (FD) bias arises. The dominant sources of the bias are reflection phase shifts from the corner cube coating and dihedral errors in the corner cube manufacture. The level at which these errors come in depends on the attributes of the metrology beam interrogating the corner cube. For reflection phase shifts the polarization of the beam matters, while the bias due to corner cube dihedral errors depends on the width of the racetrack path of the metrology beam. SIM external metrology will need to correct for these effects prior to reconstructing the truss solution from the individual gauge[†] data. The corrections are derived from a model of the metrology truss and characterization of the actual optical components.

To validate the FD bias model, a test was conducted with the Kite metrology truss testbed at JPL. The Kite testbed was built to demonstrate that the metrology truss can meet SIM error budget allocations in the presence of these field dependent errors. In 2002, the Kite testbed demonstrated that it can reach SIM "requirement" level [5] performance without correcting for the field-dependent biases. In order to reach wide-angle "goal" level performance, however, the FD bias has to be predicted from a physics-based model of the metrology gauge with parameters based on characterization of the metrology system. This bias is then removed gauge by gauge prior to obtaining a truss solution.

2. THE KITE TESTBED

The Kite testbed has been described in detail elsewhere. [1] The key attributes of Kite are that it is a planar truss with 4 fiducials interconnected by 6 metrology beams. Two of the fiducials are triple corner cubes while the other two are simple corner cubes. The test corner cube in Kite, the "ACC," is a high quality optic with surface quality better than λ/30 (P-V) over any of its facets. It is gold-coated with no overcoat. The ACC can be articulated over 6 degrees of freedom, but, for the purposes of this memo, the important degrees of freedom are the tilt and tip, which correspond to the motions of the siderostat and double corner cube on SIM. Thus, the ACC is meant to emulate the DCC mounted on each SIM siderostat. Kite's 6 legs are numbered as shown in Figure 2. Note that only legs 1, 2, and 3 see the ACC.

Figure 3 shows the QP beam launcher and the metrology beam, which is linearly polarized. Note that the metrology beam follows a racetrack. The width of this racetrack is an important parameter in predicting the error arising from corner cube dihedral errors. As seen in the figure, the beam profile is a double crescent, due to the masking of the metrology beam using a rectangular bar.

The Kite error metric, sometimes also called the "5-1" metric, is the difference between the measured length change in leg 2 and the predicted value based on the measurements of the other 5 legs:

$$\text{Kite Error Metric:} \qquad \Delta_{5-1} = g_2^{pred} - g_2^{meas} \tag{1}$$

This metric is sensitive to field dependent errors because the three incident metrology beams on the ACC have different incidence angles and hence would experience different field-dependent errors.

[†] The term gauge refers to a beam launcher plus all the associated electronics needed to measure displacements.

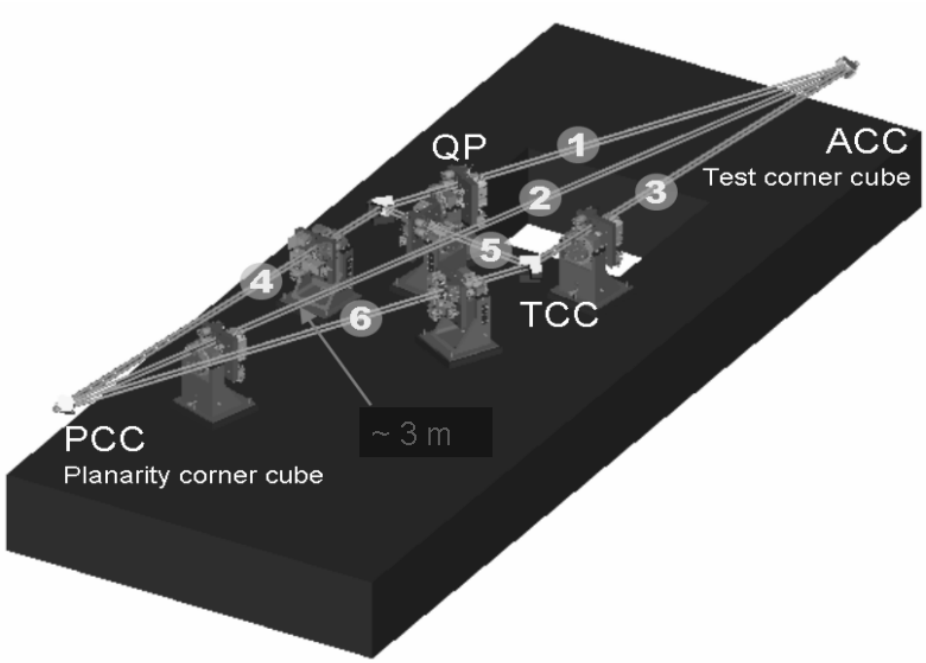

Figure 2: The Kite testbed is a 2-dimensional metrology truss, designed to demonstrate picometer external metrology for SIM.

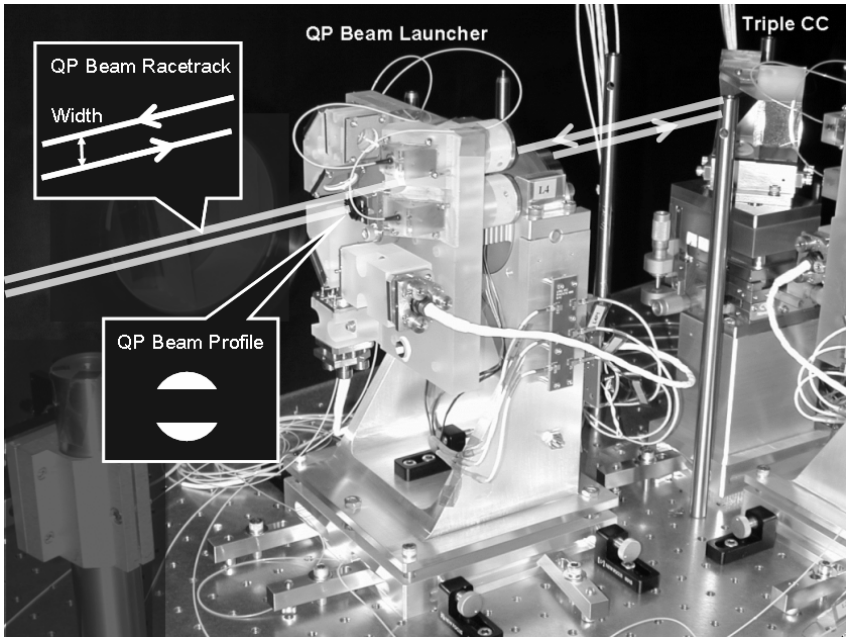

Figure 3: QP Beam Launcher in the Kite testbed. The racetrack configuration of the metrology beam is shown.

3. THE VALIDATION METRICS AND THE REQUIREMENTS

For the purposes of producing a model relevant to SIM operation, there are three model validation requirements that have been levied on the combination of Kite and its field-dependent model. These are summarized as follows:

I. The Maximum Fractional Deviation (MFD):

The first metric of model validation is the maximum fractional deviation. This is a sanity check to assure that the biases predicted in the model match what is observed in the testbed before any processing is applied which might hide gross mismatch in some attribute of the curves. This requirement states that the model and testbed results shall vary by no more than 20% of the peak-to-peak range of the bias over the wide-angle field of regard as measured by the testbed.

$$\text{Maximum Fractional Deviation} \qquad MFD \equiv \frac{\max\left(\left|T-M\right|\right)}{\left(\max\left(T\right)-\min\left(T\right)\right)} < 20\% \tag{2}$$

where $T\left(\theta,\phi\right)$ is the testbed-measured bias versus corner cube tip and tilt in the Kite "5-1" metric, and $M\left(\theta,\phi\right)$ is the same quantity predicted by the model. These functions are defined over a range spanning the SIM range of articulation in wide angle observations. Even though these quantities are called "unprocessed," it should be noted that the "raw" value of the overall offset in T has no meaning (since it comes from relative metrology) so this degree of freedom is set to zero at the center of the field of regard in both T and M.

II. The Kite testbed repeatability:

Strictly speaking, this is a testbed performance requirement and not a model match requirement. The intent is to avoid a fortuitous "match" between the model and a testbed data run, if the latter varies widely from run to run due to errors in the testbed. Hence it is required that the testbed bias be measured in multiple runs and the mean trend be used in comparing with the model. This requirement is based on the post-processed residual field-dependent bias, obtained by applying the SIM grid processing effects to the data. The precise extent and mapping of the post-processing is not yet fully resolved. Currently Kite is allowed to remove up to 7/8 of the planar trend in the field-dependence. Ideally we want to get the repeatability, over many days, of the pure field-dependent portion of the Kite error. The repeatability metric and its requirement are:

$$W = \sqrt{\frac{1}{N_{runs}N_{\theta,\phi}}\sum_{i=1}^{N_{runs}}\sum_{\theta,\phi}^{N_{\theta,\phi}}\left[R_i\left(\theta,\phi\right)-\bar{R}\left(\theta,\phi\right)\right]^2} \;<\; 70\text{ pm} \tag{3}$$

where $\bar{R}$ is the average residual field-dependence, given by:

$$\bar{R}\left(\theta,\phi\right) = \frac{1}{N_{runs}}\sum_{i=1}^{N_{runs}} R_i\left(\theta,\phi\right) \tag{4}$$

In the above equations, R_i represents the ith residual surface.

III. Testbed-Model Match-up: Here we want to know the rms difference over the WA field of regard between the average field-dependent surface (over many runs) and the model-predicted surface. The definition of the metric and the associated requirement are given by:

$$V = \sqrt{\frac{1}{N_{\theta,\phi}}\sum_{\theta,\phi}^{N_{\theta,\phi}}\left[\bar{R}\left(\theta,\phi\right)-M\left(\theta,\phi\right)\right]^2} \;<\; 78\text{ pm} \tag{5}$$

where $\bar{R}$ again is the testbed residual field dependence and M is the corresponding surface predicted by the model.

The figure below gives a simplified graphic representation of these requirements.

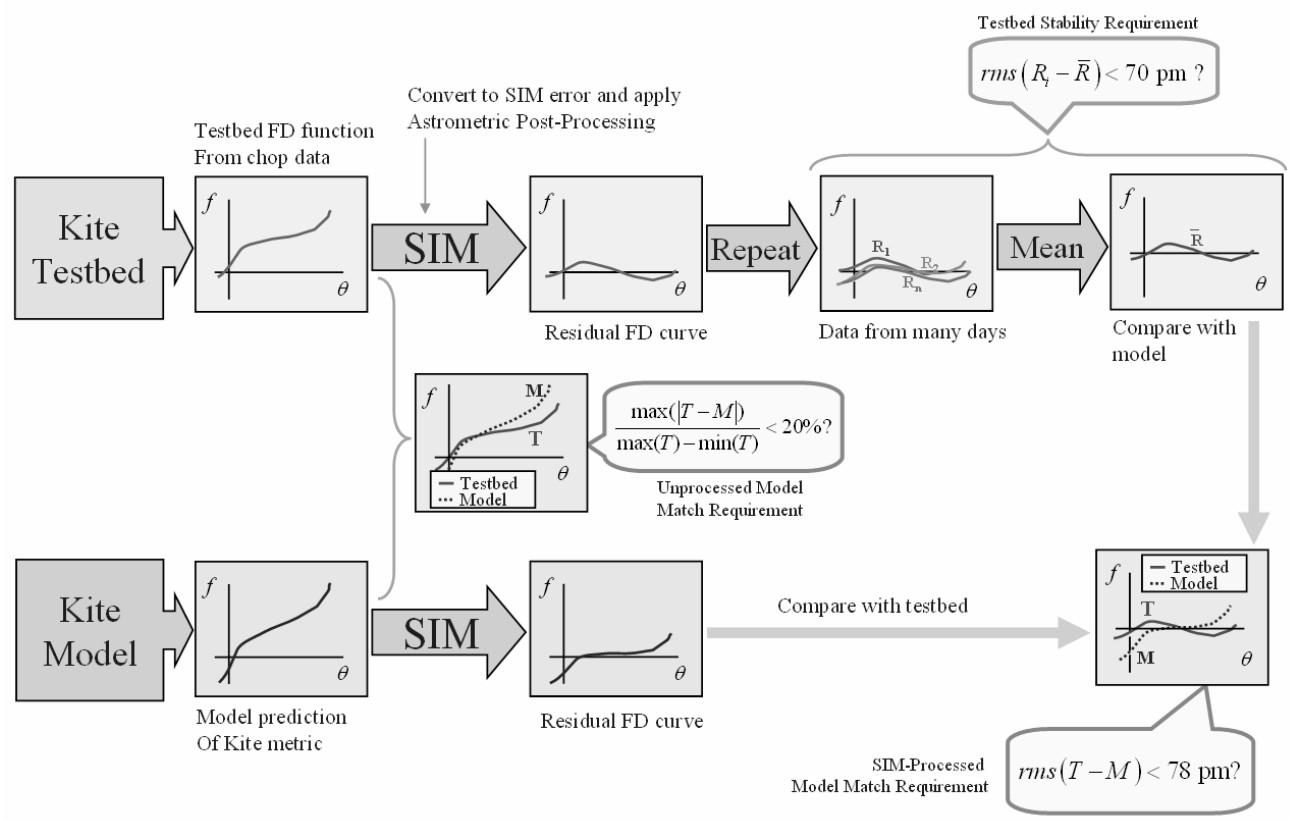

Figure 4: The three model validation criteria on the Kite testbed and its model. The average testbed field dependence is labeled T in the figure, and corresponds to the quantity in the text. The arrow labeled SIM currently corresponds to the subtraction of 7/8 of the observed plane in the field of regard.

4. THE MODEL

The heart of the Kite truss model involves a single-ray representation of a metrology gauge between two corner cube retroreflectors. This field-dependent model is physics-based, incorporating geometric ray-tracing and electric-field propagation, including Fresnel reflection coefficients at each reflecting surface. The model is implemented in MATLAB and encompasses the following physical effects:

- Geometric ray-trace for a nominal ray representing the photometric center of the metrology beam
- Dihedral angle errors in the corner cubes
- Incidence angle and incidence location of the metrology beam on each facet of each corner cube
- Polarization state of the metrology and reference beams
- Complex index of the coatings on the corner cube surfaces

The model only represents the relative change in the gauge readings (relative metrology) as the ACC is scanned over the field-of-regard (FOR). Nominal absolute metrology measurements are provided by the testbed prior to implementation of the model.

In each leg of the Kite Testbed, a single metrology gauge sits between two corner cubes. A linearly polarized metrology beam is launched from the gauge towards the first corner cube (the non-articulating corner cube in Legs 1, 2, and 3) while an identical reference beam remains inside the gauge. The metrology beam is reflected from each of the three facets of the first corner cube sequentially (i.e. the beam does not intersect a roofline) before proceeding to the second

corner cube. Following the second corner cube the beam returns to the launcher where it is interfered with the reference beam (see REF for precise details).

The Kite model simulates two distinct effects: geometric ray-trace changes and electric-field based phase delay. As the ACC is articulated over the FOR the deflected angle of the returning ray changes with respect to the constant dihedral angles and the field-dependent angle of incidence. Since we assume the ray represents a plane wave, the total change in the round trip path length is the ray-trace (or dihedral) bias. If the corner cubes are perfect and therefore have zero dihedral, there would be no field-dependent path length changes. However, since manufacturing perfect corner cubes is difficult, we are left to contend with this effect.

Computation of the OPD due to dihedral error is made by tracing the ray as it propagates from launcher to corner cube to corner cube and back to the detector (inside the launcher). The required parameters include the ray start position and direction and the vector normals of each surface (including the launch and detector surfaces). Each corner cube is made up of three surfaces where the angle between each pair is 90 degrees plus a delta angle in arcseconds. These small yet significant dihedral angles produce a field-dependent OPD bias over the field-of-regard. The relative metrology OPD is found to be

$$OPD_D = dz = L(u,v) - L(0,0)$$

where $L(u,v)$ is half of the total field-dependent path length as the ray travels from start to finish.

The start position of the ray representing the metrology beam is nominally assumed to be located at the geometric center of the metrology beam as specified in the Kite Testbed. However, it came to light that the intensity of the metrology beams were not uniform nor symmetric. Instead, there was a distinct intensity profile that shifts the centroid of the beam away from the center. Using a sliding mask it was found that the interferometric beam profile was often displaced to favor one crescent or the other (Figure 3).

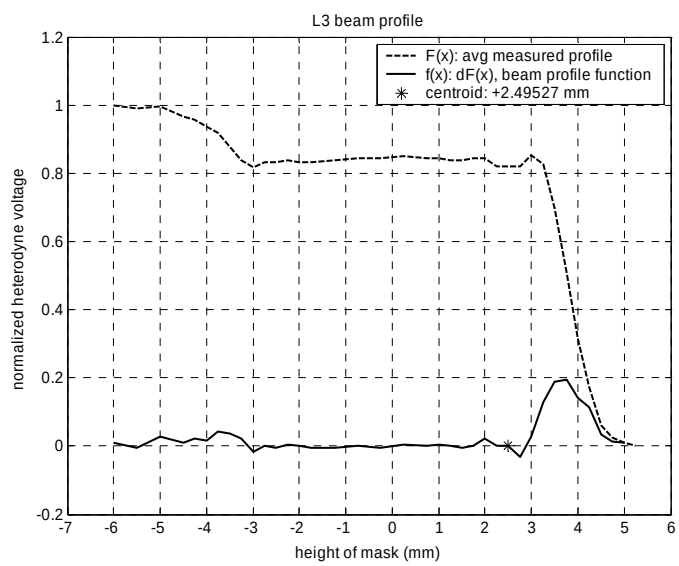

Figure 5: Calculation of the new beam centroids based on these measurements resulted in shifts in the width of the racetracks in Legs 1, 2, and 3 by -2.332mm, +3.074mm, and -4.990mm respectively. The new racetrack widths were incorporated into the model

The electric-field based phase delay effect is founded on the reflective properties of surfaces having a complex index of refraction. An electric-field incident on a surface having a complex index will experience a shift in the phase of the electric-field relative to its wavelength and the angle of incidence. The amount of phase shift changes as the angle of incidence changes. Unfortunately, the phase change as detected by our interferometric metrology gauge corresponds to a perceived change in the path length that is not separable from a real change in the distance between the two fiducials.

At any given surface there is an incident, reflected, and transmitted electric-field. It is traditional and useful to break the electric field into components parallel and orthogonal to the plane of incidence, labeled P and S, respectively. These S- and P- vectors experience different phase shifts in accordance with the Fresnel equations.

Using the convention as shown in Figure (6),

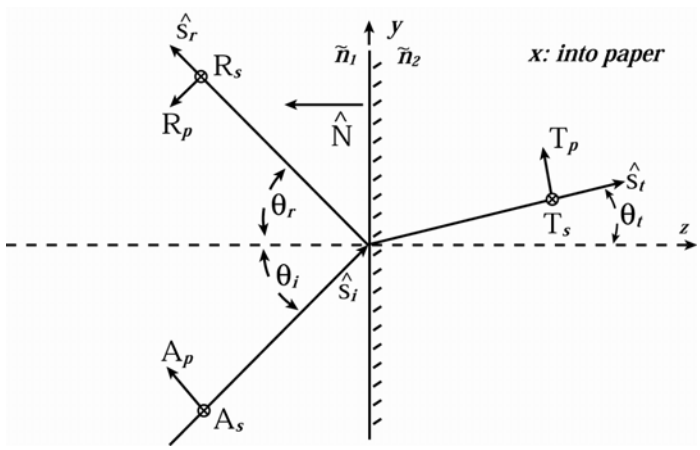

Figure 6: Reflection and transmission of an electric-field at a surface. Note the definition of S and P vectors for incident, reflected, and transmitted fields as shown here directly influence the sign of the Fresnel Reflection coefficients used in this model.

The Fresnel Reflection coefficients are [4]

$$\tilde{C}_P^{(r)} = \frac{\tilde{n}_2 \cos\theta_i - \tilde{n}_1 \cos\theta_t}{\tilde{n}_2 \cos\theta_i + \tilde{n}_1 \cos\theta_t}$$

$$\tilde{C}_S^{(r)} = \frac{\tilde{n}_1 \cos\theta_i - \tilde{n}_2 \cos\theta_t}{\tilde{n}_1 \cos\theta_i + \tilde{n}_2 \cos\theta_t}$$

where $\tilde{n}_1$ and $\tilde{n}_2$ are the refractive indices for vacuum and gold respectively.

For an incident electric-field of

$$E^{(i)} = \vec{A}_S + \vec{A}_P = A_S \hat{s}^{(i)} + A_P \hat{p}^{(i)}$$

on a surface, the reflected electric field is

$$E^{(r)} = A_S \tilde{C}_S^{(r)} \hat{s}^{(r)} + A_P \tilde{C}_P^{(r)} \hat{p}^{(r)} .$$

The Kite model tracks the surface normals and positions of each corner cube surface, the launch surface, and the detector surface as well as the polarization state of the initial metrology and reference electric-fields as the ACC is articulated over the field of regard. The incident and reflected electric-field at each surface is computed and the total change in the phase of the field at the detector is converted into units of distance based on the wavelength. It is important to note that for the phase delay calculations the propagation of the electric-field through free space is not considered, since this is already included in the geometric optical path difference model. The complex index of refraction of each bare gold reflective surface is assumed to be n = 0.419+i 8.42 for nominal gold.

The time-independent electric-field along the direction of propagation is:

$$E = E_o \exp\left(+i(k\hat{s}\cdot\vec{r} - \varphi_o)\right) = E_o \exp\left(+i(kz - \varphi_o)\right) = E_o \exp\left(+i(\frac{2\pi\tilde{n}z}{\lambda_o} - \varphi_o)\right) = E_o \exp\left(+i(\frac{2\pi(n+i\kappa)z}{\lambda_o} - \varphi_o)\right)$$

where $z = \hat{s}\cdot\vec{r}$ is the distance traveled, $\hat{s}$ is in the direction of propagation, $\vec{r}$ is the position vector, φ_o is the initial phase at $t = 0$, and $\tilde{n} = n + i\kappa$ is the complex index of refraction of the medium.

The OPD due to phase is given by

$$OPD_P = dz = \frac{\lambda_o}{2\pi n}\left(d\varphi(u,v) - d\varphi(0,0)\right)$$

where $d\varphi$ is the phase at the detector surface relative to the initial phase φ_o, and u and v are the tip and tilt angles.

The final field-dependent bias is the sum of the dihedral and refractive index effects. Sensitivity studies based on a working and experimentally validated model have shown that these two parameters are the primary contributors to field-dependent bias in single-gauge measurements.

To go from a single gauge to Kite, the FD biases in the three legs of Kite that see the test corner cube (ACC) are predicted individually using the gauge model. The prediction uses the characterization data from the Kite testbed. These predicted biases can be used two ways:

Method 1: The first approach is to directly predict the bias in the 5-1 metric by inserting the gauge model biases as the "gauge readings" for legs 1, 2, and 3, and inserting zero for legs 4, 5, 6. Using absolute metrology data from Kite, the FD bias in the 5-1 metric can then be predicted.

Method 2: The second approach is to correct the raw Kite data for each of the gauges 1, 2, and 3 with the FD bias predictions from the model appropriate to the data set being analyzed. The 5-1 metric is computed after this correction.

Of the two methods, the first has the advantage that it can be used for ex-post-facto comparisons, while the second is the more exact approach and makes no linearity assumptions. In practice, at the levels of correction we are dealing with, there should be no significant difference between the two methods.

It should also be noted that, beside the single-ray gauge model, a full ZEMAX ray trace model also exists, which adds the capability to incorporate wavefront errors in both the metrology beam and the corner cube. However, as shown in this memo, SIM requirements can be met, if sufficiently high quality corner cubes are used, without incorporating wavefront effects in the model.

5. THE KITE WIDE-ANGLE DATA

The Kite wide-angle (WA) data follows the SIM WA measurement scenario, involving 30-second "looks" separated by 15-second slews, and a total run time of one hour covering a SIM "tile", a portion of the sky spanning 7.5 degrees in radius. Figure 7 below shows the field points covered in a typical Kite WA data run.

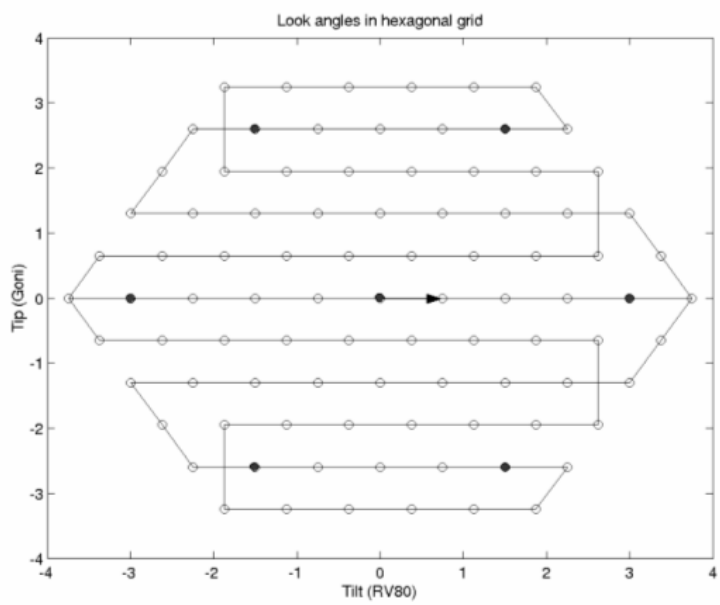

Figure 7: Example of the observing pattern in Kite all-in-one Wide-angle data.

Such a run captures both field-dependent and field-independent errors (hence referred to as an "all-in-one" test). To get the best estimate of the FD bias, Kite would have used a chopping approach (similar to NA scenarios) with timing optimized to minimize field-independent (FI) errors. Since Kite's primary objective for the past year has been to reach SIM goal-level performance in all-in-one tests, the data shown in this memo are all of this type.

The data shown here was taken over the course of a few weeks. They cover three distinct situations:

1. Nominal Configuration:

   Kite is in its nominal configuration, with the ACC 1-1-1 axis along the "spine" of the Kite, which is leg 2.

2. Clipped-beam configuration:

   Same as nominal, except that the "outer" crescent (relative to the racetrack) of the metrology beam is clipped on legs 1 and 3. This effectively reduces the racetrack width by about 6 mm. This data was available from an earlier study and was used to check that the model correctly handled the bias due to corner cube dihedral errors.

3. Mini-Grazing:

   Same as nominal, except that the ACC is clocked by 11 degrees in tilt (i.e. parallel to the Kite plane), making the incidence angles of the metrology beams on the corner cube more grazing (and more like the case in some of the legs in the SIM truss). This test brings out the effects due to reflection phase shifts, since these effects become more pronounced at grazing incidence angles.

6. COMPARISON OF MODEL PREDICTIONS WITH THE DATA

Figure 8 shows data from the nominal Kite configuration. On left is the 5-1 metric from the Kite data prior to any field-dependent processing (such as linear term removal, etc.). The only processing applied to the Kite data is the removal of a temporal drift, as measured by a number of calibrator "stars" visited at the beginning, middle, and the end of the run. On the right is the unprocessed fractional deviation (UFD), obtained by subtracting the model prediction of the field-dependent bias from the Kite data on the left, and dividing by the total range of the data over the field of regard:

$$UFD \equiv \frac{T - M}{\left(\max\left(T\right) - \min\left(T\right)\right)} \tag{6}$$

The model prediction is via Method 1 defined above, also called the direct method. The model predicts the testbed data with a maximum fractional deviation of 6%. The requirement is 20%.

The next set has data that was taken with two of the Kite legs having narrowed racetracks. This was done by blocking half of the metrology beam on legs 1 and 3. The results appear in Figure 9. Here the maximum fractional deviation is found to be about 7%.

The mini-grazing data comparison appears in Figure 10. Here the ACC is clocked by 11 degrees in tilt. The model captures this effect as well, matching the testbed data with a maximum fractional deviation of about 5%.

The Kite Wide-Angle Metric after Model Subtraction

Figure 11 shows the effectiveness of the model in predicting the field dependent bias for a variety of configurations. The tilt in the field is plotted, before and after model correction, for a number of different data runs. The first six runs are with Kite in its nominal configuration. Runs 7-9 have leg 1 (see Figure 2) with its lower crescent blocked by a mask. In run 10 both legs 1 and 3 are so blocked. Blocking a crescent changes the effective racetrack width and hence the sensitivity to dihedral errors. Runs 11-13 have the ACC starting with a tilt offset of -4 degrees, changing all the incidence angles for legs 1-3. Runs 14-16 are similar but have the ACC start with a tilt offset of +11 degrees. These runs are called "mini-grazing" because the beams are incident at near grazing angles. With the current (small) ACC, this is the most grazing incidence possible before metrology beams are clipped. Runs 17 and 18 have the ACC clocked by +3 degrees, while runs 19 and 20 have the ACC clocked by +6 degrees. Clocking the ACC also changes the incidence angles. However, it also tends to cause the metrology beams to cross corner cube roof-lines and thereby increase the error due to corner cube beamwalk. Beamwalk error prediction requires a phase map of the corner cube surface, which has not been done so far in the model, but may be added in the future.

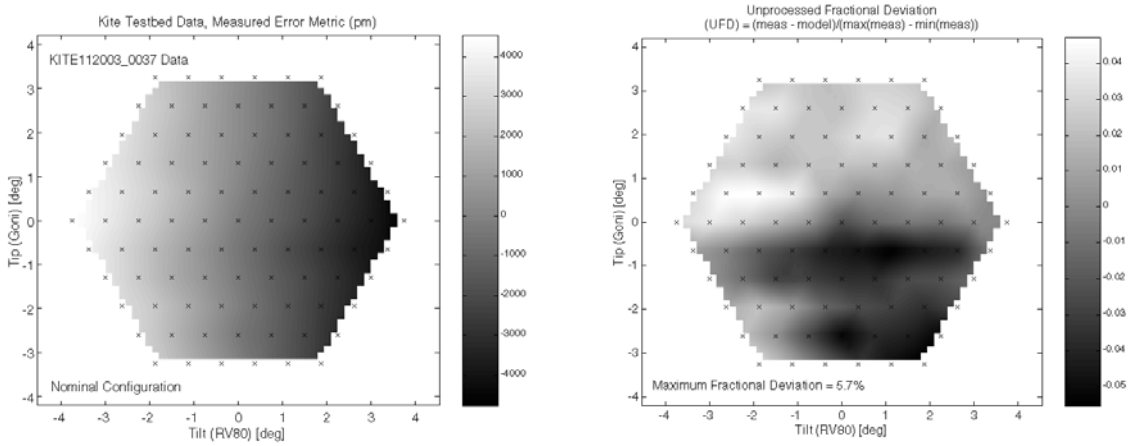

Figure 8: Kite nominal configuration model match. The raw bias in the 5-1 metric is shown on the left, while the fractional deviation is shown on the right. The MFD metric is based on the point on the left figure with the largest absolute value, that is, MFD = max(abs(UFD)). The MFD for this case is 5.7%.

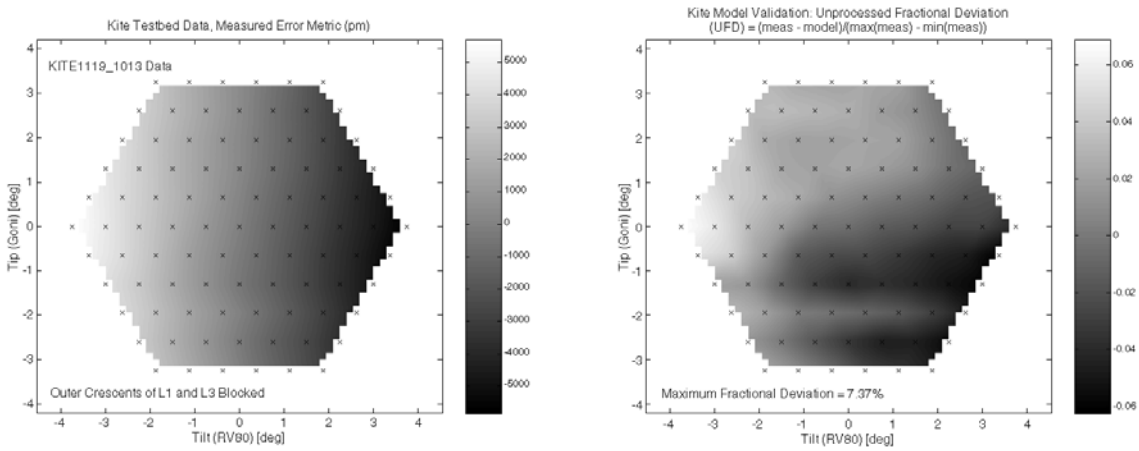

Figure 9: Kite nominal configuration but with the metrology beam outer half-crescent blocked on legs 1, 3. This changes the effective racetrack width.

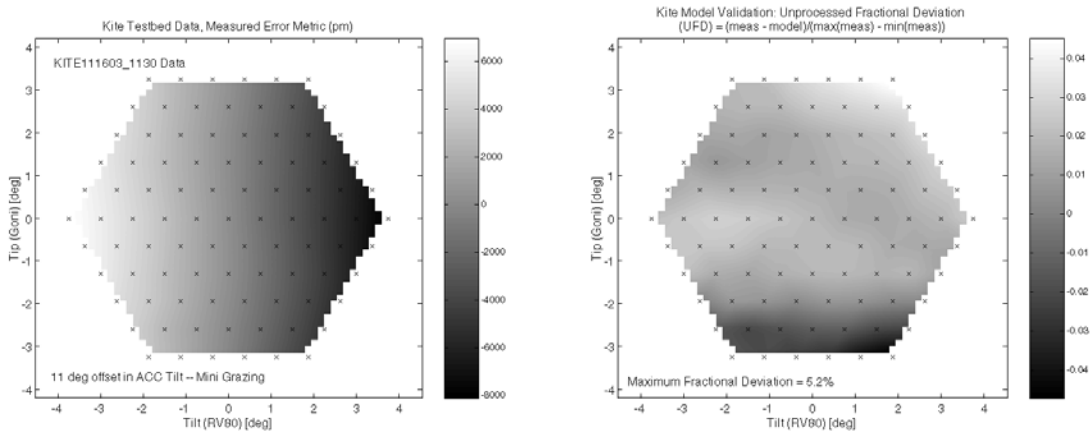

Figure 10: Mini-grazing data with ACC tilted by +11 degrees. This is a more stringent test of the model's ability to predict the bias due to corner cube complex index and metrology beam polarization.

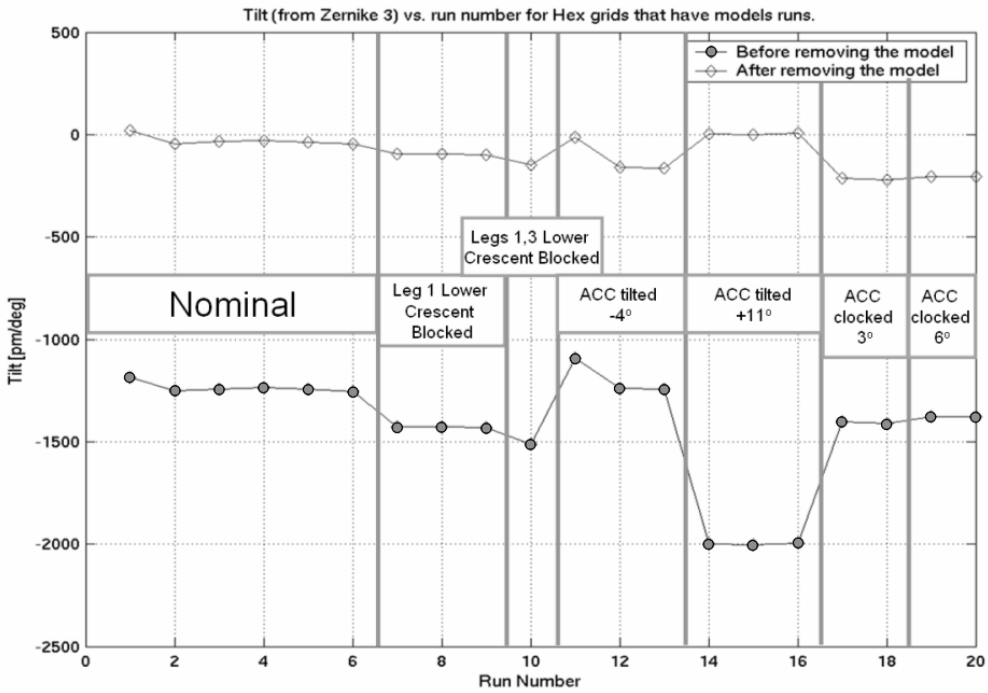

Figure 11: Tilt bias in the data before (blue) and after (red) the subtraction of the model-predicted FD bias.

7. SUMMARY AND CONCLUSIONS

A physics-based model of field-dependent biases in a metrology truss has been constructed that matches testbed measured biases at levels meeting SIM's operational requirements. The model primarily contains geometric effects (ray trace, corner cube dihedral errors) and polarization-dependent reflection phase shifts. The model relies on characterization of the testbed geometry, but not the precise determination of the actual gold coating complex indices. This model is found to match the nanometer-class bias at better than 10% for a number of different configurations. We expect that the field-dependent errors in the metrology truss can be reduced even further using actual characterized coating complex indices (via ellipsometry) and actual corner cube surface errors.

ACKNOWLEDGMENTS

The data presented in this memo was the result of diligent experimental work by the Kite testbed team and the SIM integrated modeling team at JPL. The research described in this paper was carried out at the Jet Propulsion Laboratory, California Institute of Technology, under a contract with the National Aeronautics and Space Administration.

REFERENCES

1. F.G. Dekens, O. Alvarez-Salazar, et al., "Kite: Status of the External Metrology Testbed for SIM", Proc. of SPIE conference on Astronomical Telescopes and Instrumentation, vol. 5491, (Glasgow, Scotland) June 2004. (in press)
2. M. Shao, "Science Overview of the SIM project," Proc. of SPIE conference on Astronomical Telescopes and Instrumentation, vol. 4852, (Waikoloa, Hawaii) August 2002.
3. B. Nemati, "External Metrology Truss Technology Demonstration (KITE)", Proc. of SPIE conference on Astronomical Telescopes and Instrumentation, vol. 4852, (Waikoloa, Hawaii) August 2002.
4. G.M. Kuan, R.T. Demers, "On Kite, Zemax, and Electric Field Propagation and Reflection", Internal JPL Memo, March 2004.
5. R.A. Laskin, "SIM Technology Plan: 2003 Prospectus," JPL Document D-21784, April, 2003.